TEST PROCEDURES FOR ADVANCED INSULATION PANELS

A. Hunter Fanney
Christopher A. Saunders
Stephen D. Hill
Building Environment Division
National Institute of Standards and Technology

ABSTRACT

Advanced insulation technologies are being developed in order to meet increasing stringent minimum efficiency standards for appliances and building envelopes. Numerous advanced insulation concepts have been developed to the stage that full-scale prototypes and, in some cases, commercial products are available. These concepts include powder, aerogel, foam, glass fiber filled evacuated panels, and low conductivity gas based systems, some of which are operated at a vacuum whereas others are operated at atmospheric pressure. These emerging insulation technologies offer the potential for extremely high thermal resistance values.

The National Institute of Standards and Technology (NIST) has undertaken a research program to develop thermal measurement techniques appropriate for advanced insulation panels. This paper describes the design of a calorimetric apparatus, compares the calorimetric results to measurements made using a heat flow meter apparatus for homogenous materials, and describes the procedure used to determine the thermal resistance of an advanced insulation panel. Finite-element modelling results are presented which show the effect of various physical parameters on the overall thermal resistance of a metal-clad powder-filled vacuum insulation system.

INTRODUCTION

The first guarded hot-plate apparatus at the National Bureau of Standards, the predecessor to the National Institute of Standards and Technology (NIST), was conceived and built in 1912 (Dickinson and Van Dusen 1916). Today thermal conductivity measurements are made at NIST using a 1-meter guarded hot-plate facility (Hahn et al 1974; Powell and Rennex 1982) and two commercially available heat flow meter apparatus. The primary use of the NIST 1-meter guarded hot-plate facility is to provide insulation specimens to private industry and other government laboratories for calibration purposes (NIST 1992-93). The heat flow meter apparatus, considered secondary instruments, are used to make measurements where accuracy requirements are less demanding.

Guarded hot-plates and heat flow meter apparatus are designed to measure the thermal conductivity of isotropic, homogeneous materials. ASTM Standard C-177 (ASTM 1993) , which prescribes the standard test method for guarded-hot-plate apparatus, states that testing of inhomogeneous materials can result in significant measurement errors. ASTM Standard C-177 further specifies that the surfaces of the test specimens be flat and parallel to minimize surface contact resistance. The ASTM Standard that describes the standard test for heat flow meter apparatus, C-518 (ASTM 1993), states that special care should be taken for specimens exhibiting appreciable inhomogeneities, rigidity, or especially high or low resistance to heat. Advanced insulation panels frequently exhibit one or more of these characteristics.

For example, a significant portion of the heat transfer through a metal-clad compact vacuum panel is conducted laterally along the front and rear metal faces of a panel and short circuited through its metal edges. This lateral heat transfer can result in significant measurement errors using a guarded hot plate or heat flow meter apparatus. Additionally, the insulation panels may be larger in area than the metering areas of these apparatus and may have surfaces which are neither flat nor uniform. A calorimetric measurement technique (Fang et al 1985; ASTM 1993) is presented within this paper that permits the thermal performance of this type and other advanced insulation panels to be measured.

EXPERIMENTAL APPARATUS

An experimental apparatus, Figure 1, was constructed to measure the heat transfer rate through an advanced insulation panel. The apparatus consists of a freezer, a polystrene mask which surrounds the insulation panel, and a calorimeter. The freezer maintains one side of the insulation panel at a temperature lower than laboratory ambient to ensure that the heat flows from the calorimeter through the panel and mask. The use of a mask permits the testing of various size insulation panels. The calorimeter maintains the air on the other side of the insulation panel at laboratory ambient temperature.

The doors of a commercial freezer were removed and replaced with an expanded polystyrene mask and the insulation panel being evaluated. The temperature within the freezer is controlled using a resistance heater located downstream of the evaporator coil, a temperature sensor within the freezer and a proportional-integral-derivative controller. A plenum was constructed behind the panel and mask creating a 10.2 mm-thick air channel. A variable-speed tangential fan is used to provide a uniform air velocity within the plenum. Sixteen uniformly spaced thermocouples are used to measure the air temperature within the plenum.

The calorimeter, Figure 2, is placed against the mask. The calorimeter is fabricated from two 51-mm thick layers of extruded polystyrene. An eight junction thermopile is used to measure the temperature difference across each of the four equal area side walls. The temperature difference across the back wall of the calorimeter is measured with a 16-junction thermopile. An electric resistance heater, constructed of 27 gage bare nickel chromium wire, provides the heat required to maintain the interior of the calorimeter box equivalent to laboratory ambient. The air temperature within the calorimeter is measured using 16 uniformly spaced thermocouples. Additional thermocouples are available to measure the front and rear surface temperatures of the polystyrene mask and insulation panel being evaluated. All measurement signals are fed to a data acquisition system interfaced to a personal computer. The personal computer converts the thermocouple and thermopile outputs into engineering units, records the acquired data, and controls the power supplied to the heater within the calorimeter.

TECHNICAL APPROACH

The area of the expanded polystyrene covered by the calorimeter is called the metered area, whereas the portion exterior to the calorimeter is referred to as the guard area. The mask area is the polystyrene material surrounding the test specimen within the calorimeter.

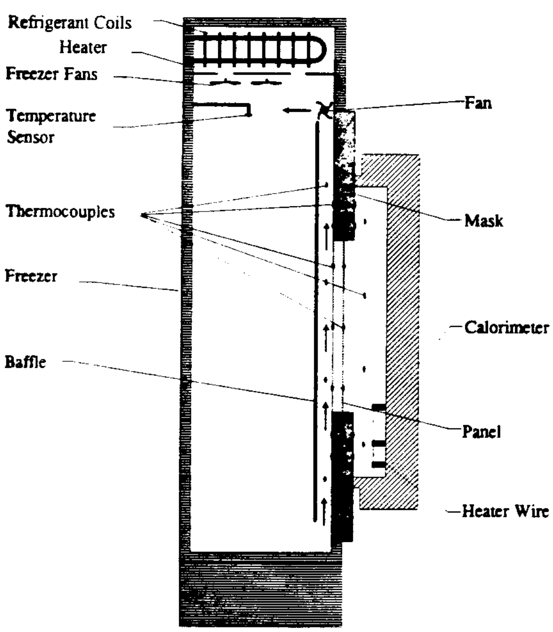

Experimental Apparatus

Figure 1

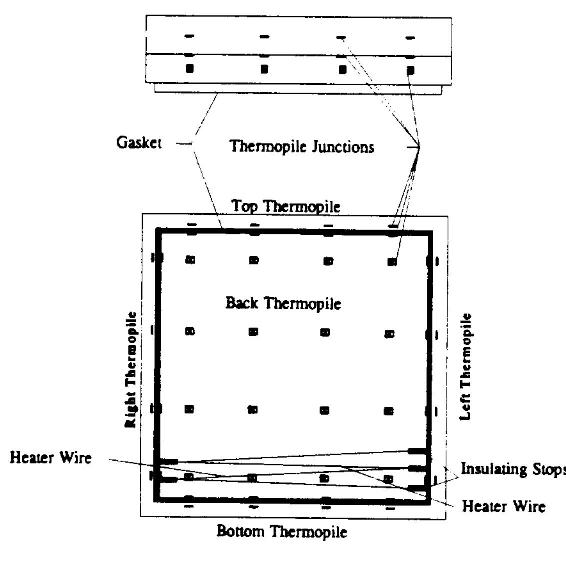

Top and Front Views of Calorimeter

Figure 2

An energy balance on the calorimeter yields

$$Q_T = Q_{IP} + Q_{SM} + Q_W \tag{1}$$

where

Q_T is the power supplied to the electric heater, W
Q_{IP} is the heat flow through the insulation panel, W
Q_{SM} is the heat flow through the surrounding mask area, W
and Q_W is the heat flow through the five calorimeter walls, W.

Here the lateral heat flow between the metered and guard area is reduced to zero by carefully matching the surface temperature at the edge of the metered area with that of the adjacent guard area (Brown and Schuyler 1979).

If the temperature within the calorimeter is held equivalent to the surrounding air temperature there is no heat transfer through the five calorimeter walls. However, this is rarely the case and therefore the heat loss through the calorimeter walls is calculated using

$$Q_W = k_c \sum_{i=1}^{5} \frac{A_i \Delta T_i}{\Delta x_i} \tag{2}$$

where k_c is the thermal conductivity of the material used to construct the calorimeter, W/m·K
A_i is the area of each calorimeter wall, m^2
ΔT_i is the measured temperature difference across each calorimeter wall, °K
and Δx_i is the thickness of each wall, m.

Thus, the heat flow through the insulation specimen and surrounding mask is

$$Q_{IP} + Q_{SM} = Q_T - k_c \sum_{i=1}^{5} \frac{A_i \Delta T_i}{\Delta x_i} \tag{3}$$

The heat flow through the insulation specimen and surrounding mask may also be expressed as

$$Q_{IP} + Q_{SM} = Q'_{IP} + Q'_{SM} + Q_D \tag{4}$$

where Q'_{IP} represents the heat transfer which would occur through the insulation panel if the mask was not present

Q'_{SM} represents the heat transfer which would occur through the mask if the insulation panel was not present

and Q_D represents the difference between the heat transfer through the combined insulation panel and surrounding mask assembly and the sum of the heat transfer through each individual component in the absence of the second component.

The quantity Q_{SM} is calculated using finite-element or finite-difference numerical techniques.

Combining equations 3 and 4

$$Q'_{IP} = Q_T - k_c \sum_{i=1}^{5} \frac{A_i\, T_i}{\Delta x_i} - Q'_{SM} - Q_D \tag{5}$$

The first three quantities on the right hand side of equation 5 are measured or calculated. The additional heat flow attributed to the panel/mask assembly compared to the sum of the heat flows through the individual components, Q_D was computed using a finite-element code. Expressing this quantity, as a function of the heat transfer through the insulation panel without a surrounding mask yields

$$\frac{Q_D}{Q'_{IP}} = \frac{(Q_{IP} + Q_{SM} - Q'_{SM}) - Q'_{IP}}{Q'_{IP}} \tag{6}$$

The thickness of the insulation panel was varied in order to assess Q_D for panels of varying overall thermal resistance. Figure 3 shows the results for a homogenous isotropic insulation panel placed within a surrounding expanded polystyrene mask. A metal-clad compact vacuum insulation panel surrounded by a polystyrene mask produced the results shown in Figure 4. Using equation 5, the term Q'_{IP} can be determined in the following manner. Initially the term Q_D is assumed to be zero yielding an initial value of Q'_{IP}. This initial value in conjunction with Q'_{SM} is used to compute the ratio R_{panel}/R_{mask} which represents the air-to-air overall thermal resistance of the panel and mask, respectively. Figure 3 or 4 is used to yield a value of Q_D for the value R_{panel}/R_{mask} and the geometry of the test configuration. Having determined the value Q_D, equation 5 is used to calculate Q'_{IP}.

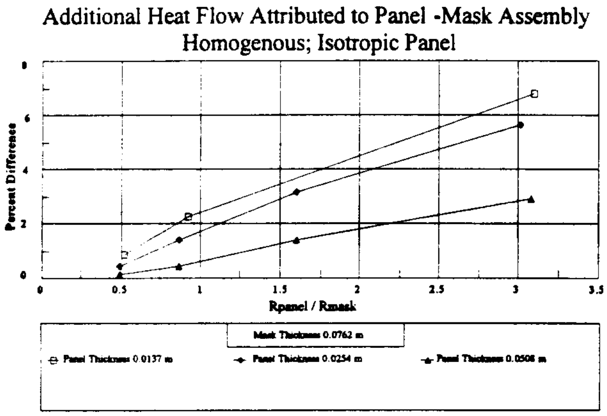

Figure 3

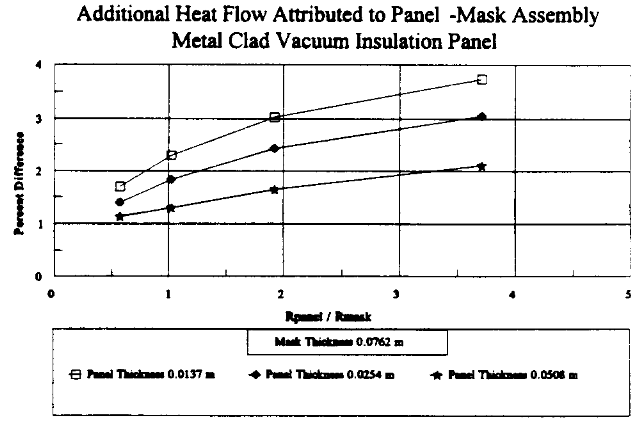

Figure 4

The overall thermal resistance of the panel is related to the heat transfer through the panel by the relationship

$$R = \frac{A_{IP} \Delta T_{aa}}{Q'_{IP}} - \frac{1}{h_c} - \frac{1}{h_f} \qquad (7)$$

where A_{IP} is the insulation panel area, m^2

ΔT_{aa} is the air temperature difference between the calorimeter interior and back (i.e., freezer-side) of the insulation panel, °C

and h_c and h_f are the overall convective film coefficients, including radiation heat transfer, for the calorimeter side and freezer side of the insulation panels, W/m$^{2\circ}$C.

EXPERIMENTAL RESULTS

Tests were initially conducted to compare the measured thermal conductivity of a homogenous material using the calorimeter apparatus to thermal conductivity measurements made using a heat flow meter apparatus that conforms to ASTM Standard C-518. Expanded polystyrene insulation specimens, 50.8 mm and 72.2 mm in thickness, were tested. The measured thermal resistivity of the expanded polystyrene specimens is shown in Figure 5 as a function of the specimen mean temperature. The squares and diamonds denote measurements made using the calorimeter and a heat flow meter apparatus, respectively. The solid lines represent a linear least squares fit regression to the calorimeter measurements. The agreement between thermal conductivity values based on the regression curve and the measurements made using the heat flow meter apparatus is within 2.5

percent. The estimated measurement uncertainty of the heat flow meter apparatus is ± 3.0 percent (Zarr 1991). Thus, the thermal conductivity measurements for the expanded polystyrene specimens using the calorimeter is within the estimated uncertainty of the heat flow meter apparatus.

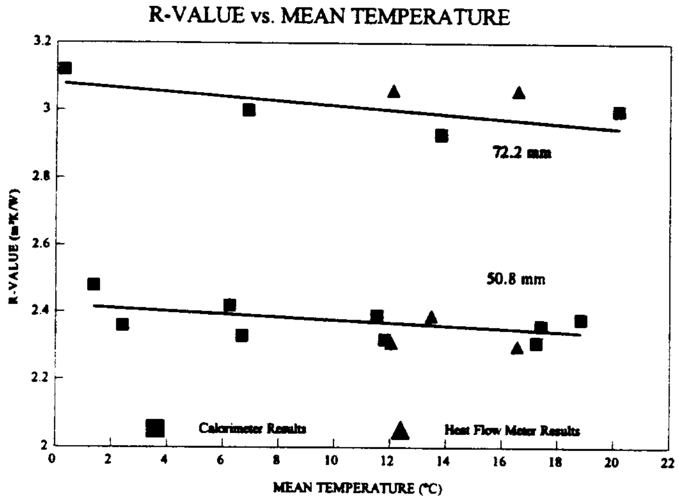

Figure 5

In order to test an advanced insulation panel, an opening was made in the center of the 76.2 mm polystyrene specimen to accommodate a nominal 13.7 mm thick metal-clad compact vacuum insulation panel. The temperature of the air passing across the rear of the panel was maintained at -7.9° C while maintaining the interior of the calorimeter at laboratory temperature, approximately 22.4° C. A five day test was conducted with measurements recorded at 30 second intervals. The measured steady state heat flow rate through the compact vacuum insulation panel and surrounding mask was 13.08 watts.

The resulting experimental data was compared to results obtained using a finite-element model. The thermal conductivity and dimensions of the materials used in the construction of the compact vacuum insulation panel are given in Table 1. The measured convective film coefficients and air temperatures on the front and rear of the panel and surrounding mask were input to the finite-element model. The predicted heat flow through the compact insulation panel and surrounding mask, 12.34 watts, is within 6 percent of the measured value, 13.08 watts. Based upon this agreement, the model was deemed adequate for conducting parametric analyses and to explore the magnitude of the term Q_D in Equation 4. The overall surface-to-surface thermal resistance for the insulation panel, determined using Figure 4 and Equation 7, is 1.12 $m^{2\circ}$C/W.

PARAMETRIC ANALYSIS

Using a commercially available finite-element code, studies were conducted to assess the effect of various parameters on the overall surface-to-surface thermal resistance of a metal-clad powder-filled vacuum insulation panel. The following table gives the baseline parameters used in the computer simulations.

Table 1 Vacuum Insulation Panel Baseline Parameters	
Panel Length - Width - Thickness	0.715 m - 0.465 m - 13.7 mm
Metal-Cladding Thickness	0.1016 mm
Metal Cladding - Powder-Fill Thermal Conductivity	17.31W/mK - 4.95 x 10^{-3} W/mK
Front - Rear Air Temperatures	25°C - -10°C
Front - Rear Convective Film Coefficients	6 $W/m^{2\circ}C$ - 12 $W/m^{2\circ}C$

Figure 6 shows the effect of metal-cladding thickness and thermal conductivity on the overall thermal resistance of the insulation panel. As expected, the performance of the vacuum insulation panel is a strong function of the metal-cladding thermal conductivity and thickness. The effect of the thermal conductivity and thickness of the powder fill within the insulation panel is given in Figure 7. It is interesting to note that unlike homogenous, isotropic materials in which the overall thermal resistance is a linear function of the material thickness, a doubling of the powder thickness results in a thermal resistance considerably less than twice the initial value. This behavior is attributed to the metal cladding which encases the powder fill.

The frontal area of the baseline panel was increased to determine the relationship between frontal area and overall thermal resistance. Unlike homogenous materials where the thermal resistance is independent of frontal area, the overall thermal resistance of the metal-clad compact vacuum insulation is a strong function of frontal area, Figure 8. This is due to the thermal shunting effect of the metal cladding. As the frontal area of the panel is increased, the ratio of the metal cross sectional area around the edge of the panel becomes a smaller percentage of the overall panel area.

The influence of convective film coefficients on the surface-to-surface overall thermal resistance of the baseline metal-clad compact vacuum insulation panel is shown in Figure 9. As a point of reference, the convective film coefficient for a vertical reflective surface ($\epsilon = 0.20$) exposed to still air is 4.20 W/m^2K (ASHRAE 1993). Variations in the convective film coefficients has a noticeable effect on the surface-to-surface thermal resistance. The variation is attributed to the temperature redistribution which occurs as the convective film coefficients are varied. For example, as the convective film coefficients increase the temperature of the warmer center portion of the metal-clad panel tends to increase the panel edge temperature resulting in increased heat transfer through the

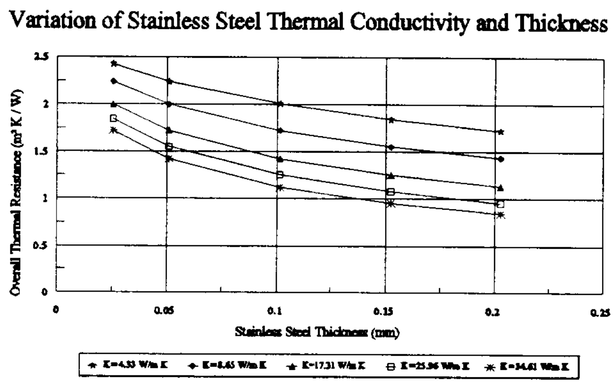

Figure 6

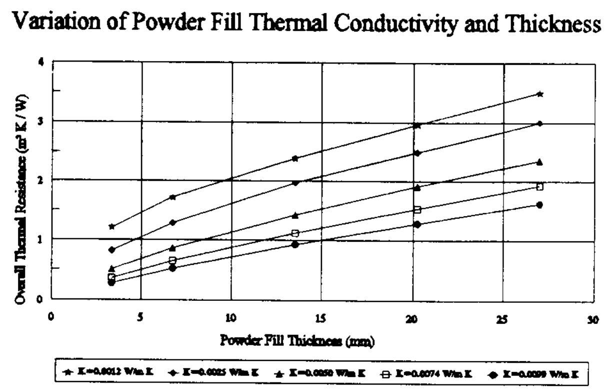

Figure 7

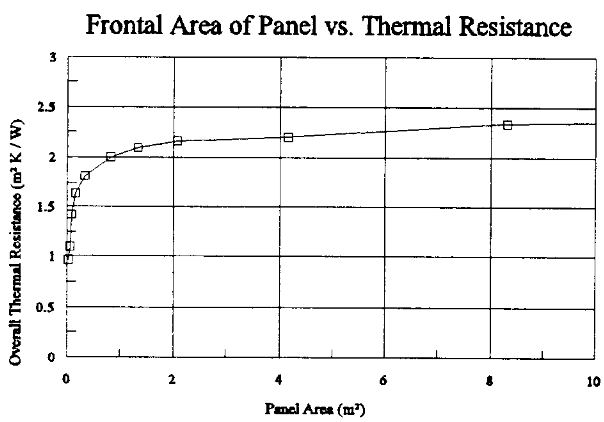

Figure 8

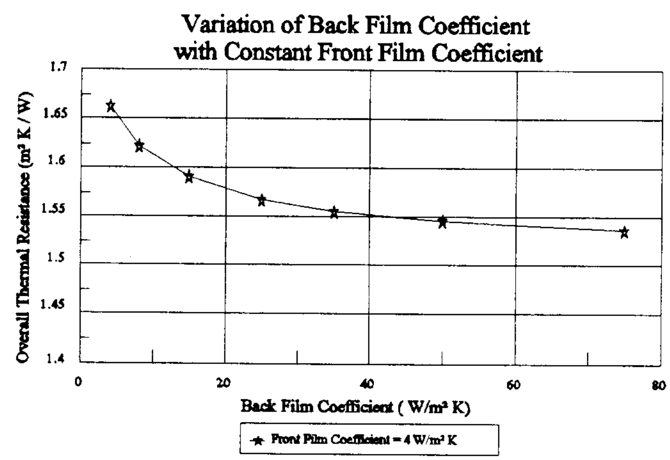

Figure 9

panel. Placing this metal-clad insulation panel in a guarded hot plate or heat flow meter apparatus, which was capable of maintaining constant surface temperatures, would be equivalent to infinite film coefficients resulting in a decrease in the surface-to-surface overall thermal resistance.

SUMMARY

A calorimetric facility has been built to measure the thermal performance of emerging advanced insulation concepts. Thermal conductivity measurement results, for homogenous isotropic specimens, are within the uncertainty of results obtained using a commercially available heat flow meter apparatus. Finite-element modelling results show that the influence of the surrounding mask on the thermal performance of the insulation panel is less than three percent for the panels considered in this study.

As expected, the performance of a metal-clad compact vacuum insulation panel is a strong function of the thermal conductivity and dimensions of the metal cladding and powder fill. An unexpected result was the strong effect that convective boundary conditions have on the overall thermal resistance of a metal-clad vacuum insulation panel.

ACKNOWLEDGEMENTS

The authors thanks Donn Ebberts for his assistance with the construction and instrumentation of the calorimeter, Robert Zarr for providing the heat flow meter apparatus thermal conductivity measurements, Doug Burch for his valuable suggestions throughout this project, and Kim Whitter for preparation of the manuscript. NIST greatly appreciates the assistance provided by John Besser of Aladdin Industries for providing the metal-clad powder-filled vacuum insulation panel used in this research project.

REFERENCES

ASTM Standard C 177-85, "Standard Test Method for Steady-State Heat Flux Measurements and Thermal Transmission Properties by Means of the Guarded-Hot-Plate Apparatus," Annual Book of ASTM Standards, Vol. 04.06. pp. 20-31.

ASTM Standard C 236-89, "Standard Test Method for Steady-State Thermal Performance of Building Assemblies by Means of a Guarded Hot Box," Annual Book of ASTM Standards, Vol. 04.06. pp. 53-67.

ASTM Standard C 518-91, "Standard Test Method for Steady-State Heat Flux Measurements and Thermal Transmission Properties by Means of the Heat Flow Meter Apparatus," Annual Book of ASTM Standards, Vol. 04.06. pp.151-162.

ASTM Standard C 976-90, "Standard Test Method for Thermal Performance of Building Assemblies by Means of a Calibrated Hot Box," Annual Book of ASTM Standards, Vol. 04.06. pp. 467-485.

Brown, W. C. and Schuyler, G. D., " A Calorimeter for Measuring Heat Flow Through Walls," Proceedings of the ASHRAE/DOE-ORNL Conference on the Thermal Performance of the Exterior Envelopes of Buildings. 1979 December. pp. 262-268.

Dickinson, H. C. and Van Dusen, M. S., "The Testing of Thermal Insulators," The American Society of Refrigerating Engineers Journal. 1916 September. Vol. 3. pp. 5-25.

Fang, J. B., Grot, R. A., and Park, H. S., "Thermal Performance of the Exterior Envelopes of Buildings III," Proceedings of the ASHRAE/DOE/BTECC Conference. 1985 December. pp. 675-688.

Hahn, M. H., Robinson, H. E., and Flynn, D. R., "Robinson Line-Heat-Source Guarded Hot Plate Apparatus," Heat Transmission Measurements in Thermal Insulations, ASTM STP 544. 1974.

NIST Standard Reference Material Catalog 1992-93, NIST Special Publication 260, N. M. Trahey, Ed. 1992 February. p. 101.

Powell, F. J. and Rennex, B. G., "The NBS Line-Heat-Source Guarded Hot Plate for Thick Materials," Proceedings of the ASHRAE/DOE Conference on the Thermal Performance of the Exterior Envelopes of Buildings - II. 1982 December. pp. 657-672.

"Thermal and Water Vapor Transmission Data," 1993 ASHRAE Handbook (SI), R. Richards, Ed. pp. 22.1-22.22.

Zarr, R. R., "Intra-Laboratory Comparison of a Line-Heat-Source Guarded Hot Plate and Heat-Flow-Meter Apparatus," Insulation Materials: Testing and Applications, 2nd Volume, ASTM STP 1116, R. S. Graves and D. C. Wysocki, Eds., American Society for Testing and Materials, Philadelphia, 1991.